PROTEINS
STRUCTURE ■ FUNCTION ■ BIOINFORMATICS

STRUCTURE NOTE

Crystal structure of *Bacillus Subtilis* CodW, a noncanonical HslV-like peptidase with an impaired catalytic apparatus

Seong-Hwan Rho,[1] Hyun Ho Park,[1] Gil Bu Kang,[1] Young Jun Im,[1] Min Suk Kang,[2] Byung Kook Lim,[2] Ihn Sik Seong,[2] Jaehong Seol,[2] Chin Ha Chung,[2] Jimin Wang,[3] and Soo Hyun Eom[1]*

[1] Department of Life Science, Cell Dynamics Research Center, Gwangju Institute of Science and Technology, Gwangju 500-712, Korea

[2] School of Biological Sciences, Seoul National University, Seoul 151-742, Korea

[3] Department of Molecular Biophysics and Biochemistry, Yale University, New Haven, Connecticut 06520

Key words: ATP-dependent protease; CodW; crystal structure; Ntn-hydrolase; autolysis.

INTRODUCTION

ATP-dependent proteases play vital roles in protein quality control and in regulating the levels of certain cellular proteins.[1–3] *Escherichia coli* and other bacteria, including *Bacillus subtilis*, contain at least three types of multimeric ATP-dependent proteases homologous to the eukaryotic 26S proteasome: Lon, Clp and HslVU.[1,2,4,5] Of these, HslVU has been extensively studied as the simplest proteasome ancestor.[6–10] Like the 26S proteasome, HslVU is comprised of two multimeric components: the ATPase HslU, which belongs to the AAA superfamily of ATPases,[11] and the peptidase HslV, which shares common structural features with the catalytic β-type subunits of the 20S proteasome. Despite a sequence identity of only about 20%, they share the amino acids crucial for proteolysis and auto-cleavage [Fig. 1(A)]. Moreover, both use a threonine residue at the N-terminus as a catalytic nucleophile exposed by the processing of a methionine residue or a prosegment upon assembly, and are thus members of the N-terminal nucleophile (Ntn)-hydrolase family.[14–16]

CodW is the proteolytic component of CodWX, which is highly homologous to HslVU[17] and has sequence identities of 52 and 55% with *E. coli* and *H. influenzae* HslV, respectively. A previous electron microscopic analysis revealed that CodW and HslV have similar molecular architectures with strict sixfold symmetry and similar dimensions (11 nm in diameter and 10 nm in height).[18] In addition, both can form a hybrid protease capable of degrading SulA, suggesting CodWX and HslVU are close relatives.[15] Nonetheless, recent biochemical studies suggest that CodW is distinct from HslV in several respects.[15,18,19] First, although CodW is synthesized as a precursor with additional residues at its N-terminus, just like proteasomal β and other HslV proteases, unlike those others CodW is incapable of autolysis before the nucleophile Thr-6 upon assembly.[15] It may be, therefore, that CodW utilizes its N-terminal serine as a catalytic nucleophile. Second, CodWX is an alkaline protease that is maximally active at pH 9.5, unlike HslUV which has a maximal activity at pH 8. Third, CodW by itself has no peptidase activity, even towards small peptides; it requires hydrolysis of ATP by CodX, which in turn leads to formation of a CodWX complex, for digestion of peptide and protein substrates. By contrast, uncomplexed HslV does show weak peptidase activity toward small peptides, and the binding of ATP is sufficient for the formation of HslVU, though ATP hydrolysis is required for the digestion of a protein substrate. This dissimilarity in the behaviors of CodW and

Grant sponsor: Korea Science and Engineering Foundation (KOSEF); Grant numbers: R01-2004-000-10936-0, R01-2007-000-10592-0 and Research Center for Biomolecular Nanotechnology (GIST).

Seong-Hwan Rho and Hyun Ho Park contributed equally to this work.

*Correspondence to: Soo Hyun Eom, Department of Life Science, Gwangju Institute of Science and Technology, Gwangju 500-712, Korea.
E-mail: eom@gist.ac.kr

Received 8 June 2007; Revised 24 July 2007; Accepted 30 July 2007
Published online 2 November 2007 in Wiley InterScience (www.interscience.wiley.com). DOI: 10.1002/prot.21758

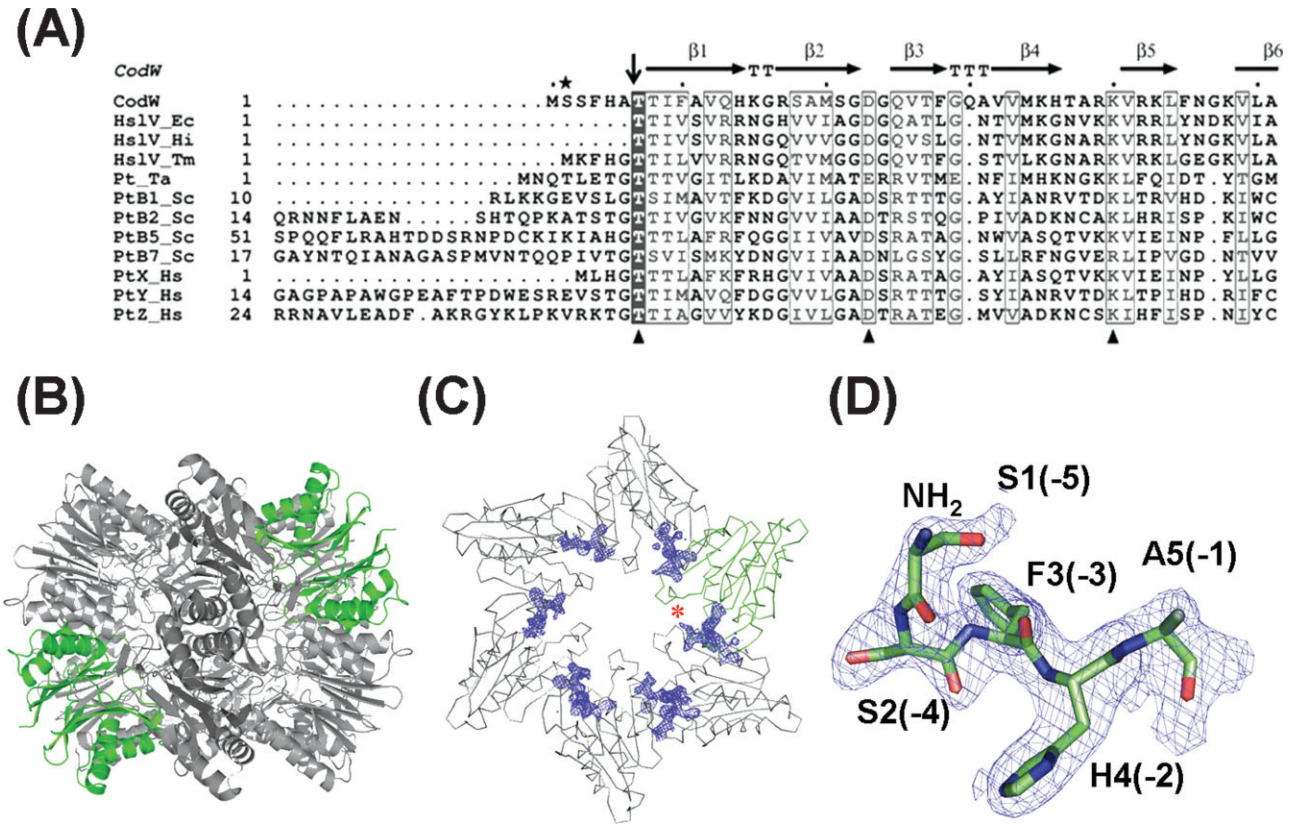

Figure 1

Crystal structure of CodW. ***A:*** *Partial sequence alignment of the precursors of 20S proteasome core particle-related proteins accomplished using the program CLUSTALX.[12] The residues considered to be crucial for proteolysis are indicated (▲): Thr-1, Asp-17 and Lys-33 in E. coli HslV; Thr-6, Asp-22 and Lys-39 in CodW.[13] A downward arrow (↓) indicates the position where autolysis occurs. The N-terminal pro-segments preceding the cleavage site are highly divergent in their lengths and sequences. The aligned sequences are as follows: CodW from B. subtilis (labeled as CodW); HslVs from E.coli, H. influenzae and T. maritima (HslV_Ec, HslV_Hi and HslV_Tm, respectively); 20S poteasome β-subunit from T. acidophilum (PTB_Ta); 20S proteasome β1, β2, β5 and β7 from S. cerevisae (PTB1_Sc, PTB2_Sc, PTB5_Sc and PTB7_Sc, respectively); 20S proteasome βX, βY and βZ form H. sapiens (PTBX_Hs, PTBY_Hs and PTBZ_Hs, respectively).* ***B:*** *Side view of one dodecamer generated by applying a crystallographic twofold operation perpendicular to the cylindrical axis of the half-dodecamer (Mol A) in the asymmetric unit. One protomer and its symmetry mate are colored green.* ***C:*** *View of the half-dodecamer (W_6) looking parallel to the molecular sixfold axis. An unbiased composite omit map contoured at 1σ (blue mesh) shows the ordered N-terminal pro-segment in each protomer. The N-terminus is located at the interface between two protomers (red asterisk).* ***D:*** *Close-up view of the pro-segment. The number in parenthesis indicates the position of the residue relative to Thr-6.*

HslV is extraordinary, since all of the catalytically important residues in HslV are well conserved in CodW. One possibility is that the observed disparities reflect sequence differences between HslV and CodW away from the conserved active site. If so, comparison of the structures of CodW and HslV should clarify the structural basis of the unique functional properties of CodW. Currently, a structure of CodW in complex with *E. coli* HslU is available.[20] This, however, diffracted poorly due to lattice translocation defects in the crystal and lacks the information necessary for comparison with other HslV structures.

Here, we describe the crystal structures of *Bacillus subtilis* CodW determined in two different space groups, $P2_1$ and $C2$, at pH 5.5 and 7.5, respectively. In both structures, the five extra N-terminal residues remain intact. This lack of autolysis can be explained by the impaired geometry of the canonical catalytic apparatus.

MATERIALS AND METHODS

Protein purification and crystallization

The protein was expressed and purified as described previously.[15] CodW protein concentrated to 5 mg/mL was crystallized at 293 K using the sitting drop vapor diffusion method. $P2_1$ crystals were obtained using a well solution of 55% (v/v) MPD, 0.1*M* sodium citrate (pH 5.5), and 8% glycerol. $C2$ crystals were obtained using a well solution of 30% (v/v) MPD and 0.1*M* HEPES-NaOH (pH 7.5) with 0.2*M* sodium citrate as a salt additive. X-ray diffraction data were collected on beam line 6B of the Pohang Accelerator Laboratory (PAL) in Korea. Taking advantage of the high concentration of MPD, crystals were directly frozen and cryo-cooled in a liquid nitrogen stream at 110 K. Data were processed using MOSFILM and SCALA software.[21] Diffraction data were

collected to a maximum resolution of 2.5 Å for *C*2 crystals and 3.0 Å for $P2_1$ crystals.

Data collection, structure determination, and refinement

Crystallographic computations were mostly carried out using the CCP4[21] and CNS[22] program packages, and model building was performed using O.[23] Molecular replacement searches using the $P2_1$ data were carried out to obtain the initial phases. The search model used was a dodecamer generated from the 1.9 Å structure of *H. influenzae* free HslV (PDB # 1G3K).[24] After 12-fold noncrystallographic symmetry (NCS) averaging and prime-and-switch phasing using RESOLVE,[25] it was evident that the Ser-1 to Ala-5 prosegment was intact in the structure. An improved electron density map around Ser-1 was computed from the *C*2 crystal data, which diffracted to a higher resolution of 2.5 Å. Combinations of protomers from the dodecameric structure determined using the $P2_1$ data set were used as search models. As a result, one half-dodecamer with a sixfold axis parallel to the *c*-axis was detected using a hexameric ring model (W_6). The other half-dodecamer molecule (W_3W_3) parallel to the *b*-axis was then manually positioned by examining the $2F_o - F_c$ Fourier map computed using the calculated phases from the first W_6 molecule. The two half-dodecameric CodW molecules in the asymmetric unit and the crystallographic dyad operation yielded the biological unit. Structural refinements with NCS restraints using CNS were conducted until convergence was obtained (R_{cryst} = 0.255, R_{free} = 0.298). A large difference in isotropic *B* factors was observed between the two half-dodecameric molecules: 50 Å^2 for W_6 and 100 Å^2 for W_3W_3. Because this implies the existence of large crystal anisotropy around a sixfold axis coincident with the crystallographic twofold-axis, 12 TLS groups assigned to each monomer were refined using REFMAC.[26] As a result, the displacement parameters, which differed significantly for the two half-dodecamers, were well accounted for by the TLS parameterization, leaving residual local displacements that were very similar between protomers and to which NCS restraints could be applied. The TLS refinement gave improvements in crystallographic *R* and free *R* factors up to 3% (R_{cryst} = 0.226, R_{free} = 0.265), and the resultant density map was also improved across the entire asymmetric unit. Solvent molecules including a Na^+ ion at the conserved cation-binding site in each CodW protomer became apparent during the later stages of refinement and were added to the model. After the structural refinement was completed using *C*2 data at a resolution of 2.5 Å, the refined structure was transported back to the $P2_1$ data at a lower resolution of 3.0 Å and further refined until no further reduction in R_{free} was observed (R_{cryst} = 0.245, R_{free} = 0.266). The data collection and refinement statistics are summarized in Table 1.

Table 1
Data Collection and Model Refinement Statistics

Crystal data	Native form I, pH 7.5	Native form II, pH 5.5
Data collection		
Space group	*C*2	$P2_1$
Unit cell dimensions		
a (Å)	185.1	78.1
b (Å)	106.8	164.4
c (Å)	152.7	95.9
β (°)	112.0	111.5
Resolution range	30.0–2.5	44.7–3.0
(last shell) (Å)	(2.54–2.50)	(3.16–3.00)
No. of observations	280,849	169,982
No. of unique reflections	90,904	44,182
Completeness (%)	95.5 (88.5)	98.1 (97.6)
Average $I/\sigma(I)$	17.2 (2.8)	7.1 (2.3)
R_{sym}[a](last shell)	0.055 (0.345)	0.089 (0.322)
Refinement		
R_{cryst}[b]	0.226	0.245
R_{free}[c]	0.265	0.266
No. of reflections (working set)	86,324	39,712
No. of reflections (test set)	4576	4438
No. of protein atoms	16,571	16,308
No. of solvent/hetero atoms	251	106
rmsd bond lengths (Å)	0.017	0.011
rmsd bond angles (°)	1.5	1.4

[a] $R_{sym} = \Sigma|I_{hkl} - \langle I_{hkl}\rangle|/\Sigma\langle I_{hkl}\rangle$, where I_{hkl} is the scaled intensity of the *hkl* reflection, and $\langle I_{hkl}\rangle$ is the mean value of the *hkl* reflection.
[b] $R_{cryst} = \Sigma|F_{obs} - F_{calc}|/\Sigma F_{obs}\rangle$, where F_{obs} and F_{calc} are the observed and calculated structure factor amplitudes of the *hkl* reflection.
[c] R_{free} was calculated in the same manner as R_{cryst}, but using the test set of reflections.

Validation and deposition

The main chain angles, calculated using PROCHECK,[27] showed that all residues fell into the most favored or additionally favored region of the Ramachandran plot. The atomic coordinates and structure factors of the *C*2 and $P2_1$ crystals have been deposited with the PDB codes 2Z3B and 2Z3A, respectively. Figures were produced using PyMOL.[28]

RESULTS AND DISCUSSION

The structure of CodW was determined in two different space groups, $P2_1$ and *C*2, at pH 5.5 and 7.5, respectively. The *C*2 structure was refined to 2.5 Å and the $P2_1$ structure to 3.0 Å. Both structures had good geometry and nearly identical quaternary arrangements: the root-mean-square deviation for the main chain atom pairs was 0.67 Å for subunit comparisons and 0.91 Å for dodecamer comparisons, with the pore-lining residues 91–93 exhibiting the largest deviations, which were greater than 1 Å.

The overall architecture of the CodW molecule is a double-doughnut-shaped dodecamer very similar to that of HslV, as was expected from the high degree of sequence conservation [Fig. 1(B,C)]. The rms deviation

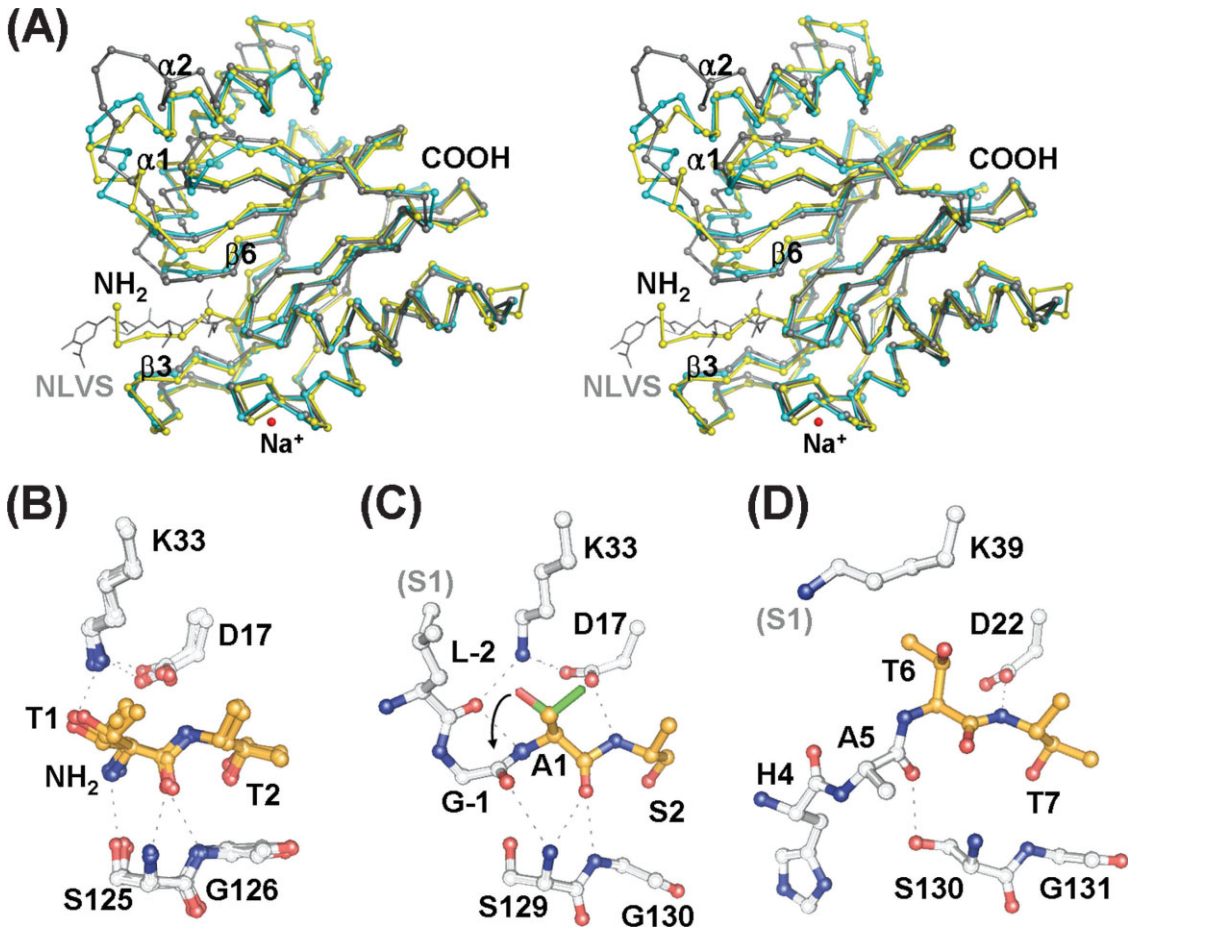

Figure 2

Structural basis for CodW's lack of autolysis. ***A:*** *Superposition of monomeric CodW (yellow) with the NLVS-complex (grey) and the free form (cyan) of H. influenza HslV (PDB #1OFI). The ordered portion of the covalently bound inhibitor 4-iodo-3-nitrophenyl-acetyl-leucinyl-leucinyl-leucinyl-vinylsulfone (NLVS) to HslV is shown as grey lines. The red sphere indicates a sodium ion bound at the conserved cation-binding site consisting of three carbonyl groups and an adjacent water molecule.* ***B:*** *Superposition of the conserved active site residues in mature proteasome β/HslV-like proteases. The active site residues from the free form (PDB #1OFH), the HslU-bound form (PDB #1OFH) of H. influenzae HslV, the free T. maritime HslV (PDB #1M4Y) and the β2-subunit of the yeast 20S proteasome (PDB #1RYP) are shown. The residues are numbered as in H. influenzae. Thr-1 and Thr-2 are colored in orange for comparison.* ***C:*** *The active site of the T1A mutant of the β1-subunit of the yeast 20S proteasome, which lacks autolysis, is shown as balls-and-sticks (PDB #1RYP). The modeled side chain of Thr-1 is drawn in green lines overlapping the side chain of Ala-1. The Leu-(-2) to Thr-1 segment shows a typical γ-turn, which ensures the addition of O^{γ} to Gly-(-1)-C.[29] The S1 substrate binding pocket is indicated in grey.* ***D:*** *The impaired geometry of the canonical catalytic apparatus in CodW is evident.*

was 1.2 Å for protomer comparisons and 1.9 Å for dodecamer comparisons between CodW and *H. influenzae* HslV (PDB #1G4A). The protomers share the typical four-layered fold exhibited by HslV and all 20S proteosome subunits; two sheets of antiparallel β-strands are sandwiched between two layers of α-helices. Each protomer includes all 180 residues and a structural Na^+ ion at the conserved cation-binding site formed by three main chain carbonyl oxygen atoms from residues 164, 167, and 170 [Fig. 2(A)]. The mean distance between the metal ion and oxygen atoms in our structure was 2.43 Å, which is nearly identical to the value observed in the *T. maritima* HslV structure.[10,30]

The composite omit map shows a clear density consistent with an N-terminal prosegment containing Ser-1, Ser-2, Phe-3, His-4, and Ala-5 [Fig. 1(C,D)]. The backbone atoms of the Ser-2 to His-4 segment form antiparallel β-sheet hydrogen bonds with strand β3. The prosegment appears to be intact in every protomer in the asymmetric unit, unlike in the quintuple mutant of the β6-subunit of yeast 20S proteasome or *T. maritima* HslV, which was found to be partially processed.[31] In CodW, the average main chain *B*-factor of the pro-segment (45 $Å^2$) was lower than that of the whole chain (51 $Å^2$). Moreover, the CodW protein was eluted in fractions with a size of ∼240 kDa on gel filtration chromatography,

which corresponds to the size of the dodecamer, and was detected as a single band on SDS-PAGE.[15] The prosegment occupies the cleft corresponding to the substrate-binding site in HslV and the catalytic proteasomal β-subunits [Fig. 2(A)].

CodW has all the conserved residues known to be crucial for proteolysis, including Thr-6, Asp-22, Lys-39, Ser-130, and Gly-131 [Fig. 2(D)]. Within the 20S proteasome, every β-subunit contains these conserved residues and is processed through autolysis, which leads to activation.[13,31,32] Indeed, the mechanism of autolysis is highly correlated with that of proteolysis. In this context, CodW's lack of autolysis is unusual, since at the sequence level CodW appears to meet all the requirements for proteolysis. On the other hand, a comparison of the geometries of the conserved active sites in CodW and the 20S proteasome/HslV-like proteases provides a clue as to why CodW does not self-cleave at the C—N bond between Ala-5 and Thr-6. In yeast proteasomal β-subunits, the catalytic apparatus includes Thr-1, Asp-17, and Lys-33 (Thr-1, Asp-17, and Lys-33 in *H. influenzae* HslV). Although this is analogous to the catalytic triad seen in serine proteases, it differs in that the N-terminal amino group and a catalytic water molecule act as a proton acceptor in proteolysis and autolysis, respectively.[8,14,31] Superposition of the active site residues in HslV and those in the mature yeast proteasomal β2-subunit shows that the geometry of the active site is maintained precisely [Fig. 2(B)]. Even in *H. influenzae* HslV, whose activation processing by HslU is accompanied by a conformational change around the substrate binding cleft,[33] the positions of the active site residues are almost invariant during activation. The conserved hydrogen-bonding pattern between Thr-1 and the Ser-125/Gly-126 segment appears to serve as a stabilizing factor for Thr-1 at this position, since the turn segment containing the conserved Ser and Gly residues (Ser-130 and Gly-131 in CodW) is the most rigid part of the structure with the lowest average *B*-factors.

In that context, the crystal structures reveal that CodW has an impaired catalytic apparatus. Most importantly, Thr-6 is shifted by ~3 Å from its expected position, which displaces the side chain of Lys-39 into an outwardly oriented position [Fig. 2(D)]. The same type of impaired geometry of the catalytic apparatus also was seen in the quintuple reactivation mutant of the yeast proteasomal β6-subunit,[31,34] where deviation of Thr-1 from its usual position in the active subunit prevents the Lys-33-N^{ζ} and a catalytic water molecule from staying in the vicinity of Thr-1. Interestingly, this mutant was still capable of partial autolysis, perhaps because the active site residues could spontaneously recover the functional geometry. By contrast, CodW exhibits no autolytic activity, implying the impaired catalytic apparatus of CodW is not spontaneously recoverable.

In their description of the structure of the T1A mutant of the yeast proteasomal β1-subunit, Ditzel *et al.* suggested that the formation of a γ-turn by the Leu-(-2) to Thr-1 segment is one of the major conformational constraints on self-cleavage.[29] In their model, Thr-1-O^{γ} would be centrally positioned over the three-residue γ-turn and attack the carbonyl carbon of Gly-(-1) [Fig. 2(C)], which means that the right conformation of the prosegment with respect to Thr-1-O^{γ} is also essential for autolysis. In the structure of the proteasomal β1-subunit T1A mutant, the S1 specificity pocket accommodates the hydrophobic side chain of Leu-(-2) and helps to form a bulge at the Leu-(-2) to Thr-1 segment. The corresponding pocket within the structure of CodW is occupied by Lys-39, which is displaced from the active site by Thr-6 [Fig. 2(D)]. Consequently, His-4 at position -2 is displaced from the pocket and stacked against Tyr-169. Apparently, the dislocation of His-4 brings about the extension of the prosegment and prevents the formation of a γ-turn at the His-4 to Thr-6 segment. It is noteworthy that the β6-subunit reactivation mutant shows blurred electron density at residues Asn-(-2) and Gly-(-1), which implies an inherent conformational flexibility in this region. We suggest that autolysis would take place in the reactivation β6-subunit mutant whenever the conformation of the Asn-(-2) to Thr-1 segment meets the structural constraints for autolysis, that is, when it forms a γ-turn. However, the crystal structure of CodW shows neither a γ-turn nor a sign of conformational flexibility at the His-4(-2) to Thr-6 segment [Fig. 2(D)]. Therefore, the spontaneous formation of a functional canonical active site via autolysis must overcome a much higher energy barrier in CodW.

Several lines of biochemical evidence imply that Ser-1 is the N-terminal catalytic nucleophile in CodW.[15,18] In the present study, however, the unambiguous density denoting Ser-1-O^{γ} is located at the cleft formed between two protomers and is close to the entrance of the proteolytic chamber, but it shows no relevant interaction with neighboring residues. This may be attributable to the low pH of the crystallization buffer. In fact, CodWX becomes inactive at pH 5.5. Otherwise, a significant conformational rearrangement around the active site would be inevitable upon activation by CodX.

The interiors of the catalytic chambers of the proteolytic components of HslV, ClpP, and the 20S proteasome are hydrophobic and favor denatured polypeptide chains (data not shown).[35] By contrast, the catalytic chamber of CodW is strongly basic, but it is apparent that the chamber will become less polar at pH 9.5, where CodW has its maximal activity. The entrance to the proteolytic chamber of CodW is formed by a hydrogen-bonded turn and a short 3_{10}-helix and contains a cluster of conserved positively charged residues, Lys-92, Arg-95, and Lys-96 (Arg-86, Arg-89, and Arg-90 in *E. coli* HslV), whose functions are not yet clear. The average diameter of the pore, which measures 20.5 Å between C^{α} atoms, is narrow enough to prevent folded proteins from reaching the

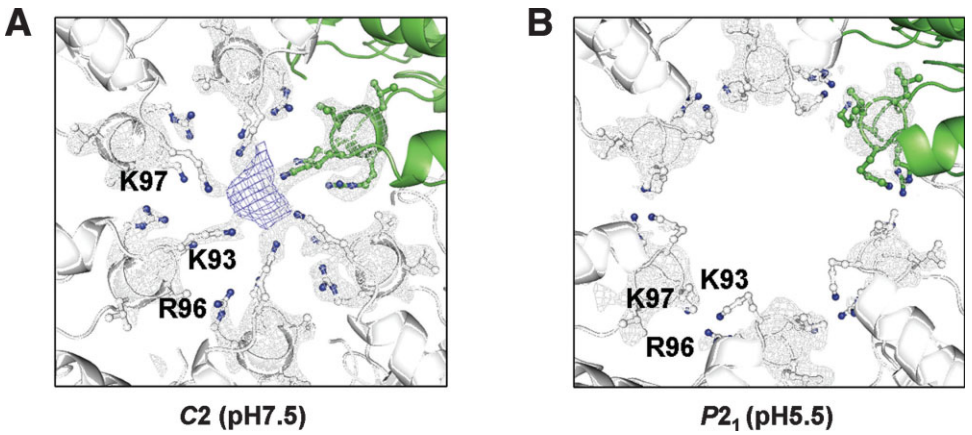

Figure 3

Obstruction of the pore leading to the proteolytic core by Lys-92. ***A:*** *A $2F_o - F_c$ map contoured at 0.8σ within 2 Å from the pore-lining residues is overlaid on the structure (grey mesh). A $F_o - F_c$ map contoured at 3σ shows an unidentified poly-anion from either the co-purification or crystallization buffer at the sixfold symmetry axial pore (blue mesh).* ***B:*** *Disordered side chains of the pore-lining residues in the $P2_1$ crystal.*

proteolytic core. The average diameter of the pore is nearly same in the *E. coli, H. influenzae* and *T. maritime* enzymes, but it changes slightly upon HslU binding.[24,36] It has been suggested that this "gating" motion is an allosteric activation/inactivation mechanism of HslV by HslU and is analogous the activation mechanism in yeast proteasomes. However, the conformational change at the pore entrance reportedly has no relation to the activation of HslV, and thus its function remains to be discovered.[37]

Although the pore leading the proteolytic core of CodW remains open in the $P2_1$ structure, in the $C2$ structure it is blocked by the presence of a poly-anion interacting with Lys-92 in each protomer [Fig. 3(A,B)]. Though presumed to be a citrate ion, the identity of the poly-anion remains unidentifiable because of the rotational averaging of sixfold symmetry. It is also unclear how many of the Lys-92 residues in the six protomers have an extended conformation to simultaneously coordinate the anion. It is noteworthy that this type of interaction has not been seen in any other HslV structure.

In HslUV/proteasome-like proteases, unfolding and translocation of the polypeptide are mediated by the ATPase subunit, and the unfolded chain is transported to the protease subunit in a vectorial fashion.[38] A denatured polypeptide chain traveling from the outlet of the ATPase subunit to the active site in the proteolytic chamber can be regarded as a random flight chain with a free end. If some structural elements were to bias the random walk of the polypeptide chain, the efficiency of the translocation of the substrate to the active site cleft would be greatly improved. In fact, the possible existence of a ratcheting mechanism directing substrates to the proteolytic chamber has been anticipated.[39] The antechambers of the 20S proteasome, which each have a volume of ~59 nm^3, may provide an example, as they must be able to maintain the polypeptide in an unfolded form as it passes through them. Prokaryotic HslV proteins do not have these antechambers. Instead, they have a flexible insertion containing a cluster of conserved positively charged residues. Moreover, the removal of a positive charge or the introduction of a negative charge at Arg-86 of *E. coli* HslV inactivates the enzyme,[40] which implies that this residue interacts with the substrate polypeptide and that its electrostatic nature is important in the translocation of the substrate. Interestingly, the Δ86–91 mutant was found to be functionally indistinguishable from wild-type enzyme,[40] which means the pore-lining segment likely facilitates substrate translocation in a passive manner. In CodW, the Lys-92 residues in some of the six protomers likely constitute a binding site for the C-terminal carboxylate of the substrate.

The study presented here revealed the intact structure of the N-terminal prosegment of CodW and showed that its lack of autolysis can be attributable to the impaired geometry of its catalytic apparatus. However, the structures failed to clarify the catalytic mechanism of CodW. Although Ser-1 was previously proposed to be an N-terminal nucleophile, the local structure around it does not provide all the required features of the active site of a protease. Furthermore, restoration of the canonical active site and subsequent autolysis will require input of additional energy to overcome the conformational constraints observed in the current structures. The activation of CodW thus appears to be accompanied by a conformational change either in the canonical catalytic apparatus or Ser-1. It therefore seems plausible that the binding of CodX is critical to the activation of CodW. In sum-

mary, the formation of a functionally active site within CodW appears to be tightly coupled to an energy-consuming activation process, which is in turn to ATP hydrolysis by CodX. The detailed mechanism will need to be explored when the structure of the CodWX complex becomes available.

REFERENCES

1. Maurizi MR. Proteases and protein degradation in *Escherichia coli*. Experientia 1992;48:178–201.
2. Gottesman S, Maurizi MR, Wickner S. Regulatory subunits of energy-dependent proteases. Cell 1997;91:435–438.
3. Wickner S, Maurizi MR, Gottesman S. Posttranslational quality control: folding, refolding, and degrading proteins. Science 1999;286: 1888–1893.
4. Goldberg AL. The mechanism and functions of ATP-dependent proteases in bacterial and animal cells. Eur J Biochem 1992;203:9–23.
5. Chung CH. Proteases in *Escherichia coli*. Science 1993;262:372–374.
6. Yoo SJ, Seol JH, Shin DH, Rohrwild M, Kang MS, Tanaka K, Goldberg AL, Chung CH. Purification and characterization of the heat shock proteins HslV and HslU that form a new ATP-dependent protease in *Escherichia coli*. J Biol Chem 1996;271:14035–14040.
7. Bochtler M, Ditzel L, Groll M, Huber R. Crystal structure of heat shock locus V (HslV) from Escherichia coli. Proc Natl Acad Sci USA 1997;94:6070–6074.
8. Bochtler M, Ditzel L, Groll M, Hartmann C, Huber R. The proteasome. Annu Rev Biophys Biomol Struct 1999;28:295–317.
9. Rohrwild M, Coux O, Huang HC, Moerschell RP, Yoo SJ, Seol JH, Chung CH, Goldberg AL. HslV-HslU: a novel ATP-dependent protease complex in *Escherichia coli* related to the eukaryotic proteasome. Proc Natl Acad Sci USA 1996;93:5808–5813.
10. Song HK, Bochtler M, Azim MK, Hartmann C, Huber R, Ramachandran R. Isolation and characterization of the prokaryotic proteasome homolog HslVU (ClpQY) from Thermotoga maritima and the crystal structure of HslV. Biophys Chem 2003;100:437–452.
11. Vale RD. AAA proteins. Lords of the ring. J Cell Biol 2000;150:F13–F19.
12. Thompson JD, Gibson TJ, Plewniak F, Jeanmougin F, Higgins DG. The CLUSTAL_X windows interface: flexible strategies for multiple sequence alignment aided by quality analysis tools. Nucleic Acids Res 1997;25:4876–4882.
13. Heinemeyer W, Fischer M, Krimmer T, Stachon U, Wolf DH. The active sites of the eukaryotic 20 S proteasome and their involvement in subunit precursor processing. J Biol Chem 1997;272:25200–25209.
14. Kisselev AF, Songyang Z, Goldberg AL. Why does threonine, and not serine, function as the active site nucleophile in proteasomes? J Biol Chem 2000;275:14831–14837.
15. Kang MS, Lim BK, Seong IS, Seol JH, Tanahashi N, Tanaka K, Chung CH. The ATP-dependent CodWX (HslVU) protease in *Bacillus subtilis* is an N-terminal serine protease. EMBO J 2001;20:734–742.
16. Bogyo M, McMaster JS, Gaczynska M, Tortorella D, Goldberg AL, Ploegh H. Covalent modification of the active site threonine of proteasomal β subunits and the *Escherichia coli* homolog HslV by a new class of inhibitors. Proc Natl Acad Sci USA 1997;94:6629–6634.
17. Slack FJ, Serror P, Joyce E, Sonenshein AL. A gene required for nutritional repression of the *Bacillus subtilis* dipeptide permease operon. Mol Microbiol 1995;15:689–702.
18. Kang MS, Kim SR, Kwack P, Lim BK, Ahn SW, Rho YM, Seong IS, Park SC, Eom SH, Cheong GW, Chung CH. Molecular architecture of the ATP-dependent CodWX protease having an N-terminal serine active site. EMBO J 2003;22:2893–2902.
19. Seong IS, Kang MS, Choi MK, Lee JW, Koh OJ, Wang J, Eom SH, Chung CH. The C-terminal tails of HslU ATPase act as a molecular switch for activation of HslV peptidase. J Biol Chem 2002;277:25976–25982.
20. Wang J, Rho SH, Park HH, Eom SH. Correction of X-ray intensities from an HslV-HslU co-crystal containing lattice-translocation defects. Acta Crystallogr D Biol Crystallogr 2005;61 (Part 7):932–941.
21. Bailey S. The CCP4 suite: programs for protein crystallography. Acta Crystallogr D Biol Crystallogr 1994;50 (Part 5):760–763.
22. Brunger AT, Adams PD, Clore GM, DeLano WL, Gros P, Grosse-Kunstleve RW, Jiang JS, Kuszewski J, Nilges M, Pannu NS, Read RJ, Rice LM, Simonson T, Warren GL. Crystallography & NMR system: a new software suite for macromolecular structure determination. Acta Crystallogr D Biol Crystallogr 1998;54 (Part 5):905–921.
23. Jones TA, Zou JY, Cowan SW, Kjeldgaard M. Improved methods for building protein models in electron density maps and the location of errors in these models. Acta Crystallogr A 1991;47 (Part 2):110–119.
24. Sousa MC, Trame CB, Tsuruta H, Wilbanks SM, Reddy VS, McKay DB. Crystal and solution structures of an HslUV protease-chaperone complex. Cell 2000;103:633–643.
25. Terwilliger TC. Maximum-likelihood density modification. Acta Crystallogr D Biol Crystallogr 2000;56 (Part 8):965–972.
26. Winn MD, Isupov MN, Murshudov GN. Use of TLS parameters to model anisotropic displacements in macromolecular refinement. Acta Crystallogr D Biol Crystallogr 2001;57 (Part 1):122–133.
27. Laskowski RA, MacArthur MW, Moss DS, Thornton JM. PROOCHECK: a program to check the stereochemical quality of protein structures. J Appl Crystallogr 1993;26:283–291.
28. DeLano WL. The PyMOL User's manual. San Carlos, CA, USA: DeLano Scientific; 2002.
29. Ditzel L, Huber R, Mann K, Heinemeyer W, Wolf DH, Groll M. Conformational constraints for protein self-cleavage in the proteasome. J Mol Biol 1998;279:1187–1191.
30. Harding MM. Metal-ligand geometry relevant to proteins and in proteins: sodium and potassium. Acta Crystallogr D Biol Crystallogr 2002;58 (Part 5):872–874.
31. Groll M, Heinemeyer W, Jager S, Ullrich T, Bochtler M, Wolf DH, Huber R. The catalytic sites of 20S proteasomes and their role in subunit maturation: a mutational and crystallographic study. Proc Natl Acad Sci USA 1999;96:10976–10983.
32. Gille C, Goede A, Schloetelburg C, Preissner R, Kloetzel PM, Gobel UB, Frommel C. A comprehensive view on proteasomal sequences: implications for the evolution of the proteasome. J Mol Biol 2003;326:1437–1448.
33. Sousa MC, Kessler BM, Overkleeft HS, McKay DB. Crystal structure of HslUV complexed with a vinyl sulfone inhibitor: corroboration of a proposed mechanism of allosteric activation of HslV by HslU. J Mol Biol 2002;318:779–785.
34. Groll M, Ditzel L, Lowe J, Stock D, Bochtler M, Bartunik HD, Huber R. Structure of 20S proteasome from yeast at 2.4 Å resolution. Nature 1997;386:463–471.
35. Wang J, Hartling JA, Flanagan JM. The structure of ClpP at 2.3 Å resolution suggests a model for ATP-dependent proteolysis. Cell 1997; 91:447–456.
36. Wang J, Song JJ, Franklin MC, Kamtekar S, Im YJ, Rho SH, Seong IS, Lee CS, Chung CH, Eom SH. Crystal structures of the HslVU peptidase-ATPase complex reveal an ATP-dependent proteolysis mechanism. Structure 2001;9:177–184.
37. Kwon AR, Kessler BM, Overkleeft HS, McKay DB. Structure and reactivity of an asymmetric complex between HslV and I-domain deleted HslU, a prokaryotic homolog of the eukaryotic proteasome. J Mol Biol 2003;330:185–195.
38. Navon A, Goldberg AL. Proteins are unfolded on the surface of the ATPase ring before transport into the proteasome. Mol Cell 2001;8:1339–1349.
39. Baumeister W, Walz J, Zuhl F, Seemuller E. The proteasome: paradigm of a self-compartmentalizing protease. Cell 1998;92:367–380.
40. Ramachandran R, Hartmann C, Song HK, Huber R, Bochtler M. Functional interactions of HslV (ClpQ) with the ATPase HslU (ClpY). Proc Natl Acad Sci USA 2002;99:7396–7401.